微型生物燃料電池

An Autonomous CO_2 Discharge and Electrolyte Agitation Scheme for Portable Microbial Fuel Cells

以微生物為觸媒，催化自葡萄糖產生質子與電子的燃料電池反應，並藉由表面張力與浮力的作用將二氧化碳廢氣排出，同時引發對流以加速電子與質子的傳遞，提高能量轉換的效率。相較於一般生物燃料電池，本研究已完成的雛型可連續操作四小時，並產生五倍以上的功率輸出，六個單元串連並可加強電壓以驅動發光二極體。

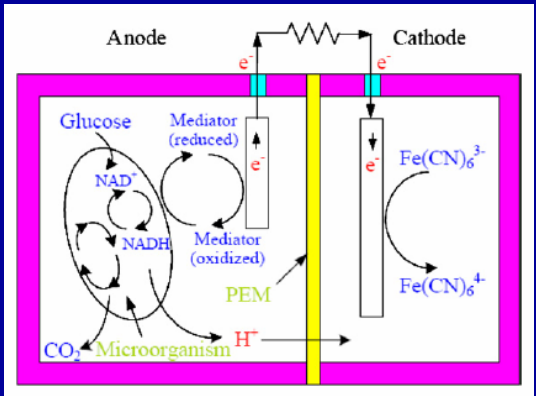

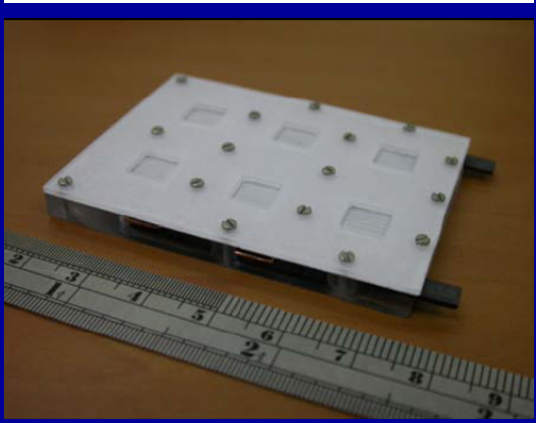

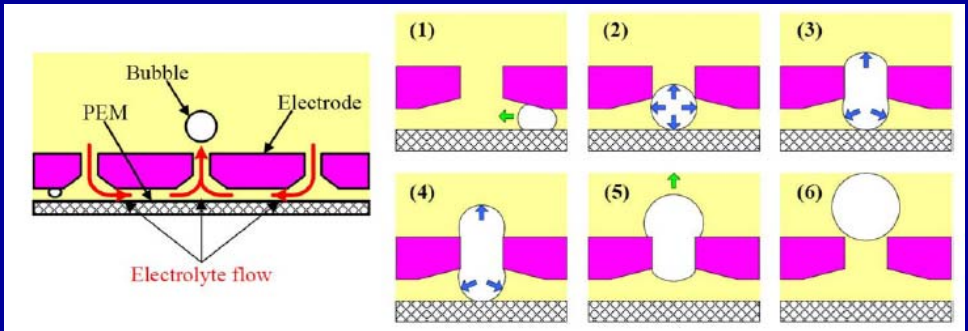

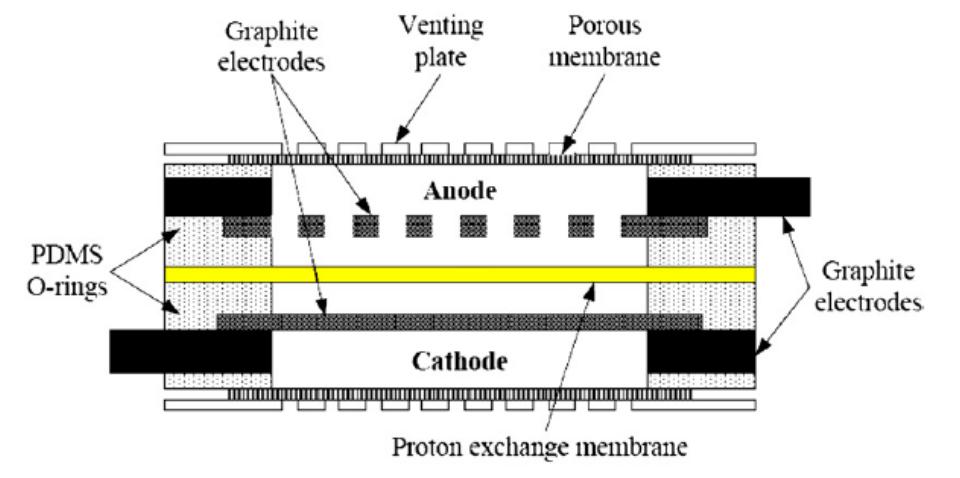

IOP Publishing Journal of Micromechanics and Microengineering
J. Micromech. Microeng. **17** (2007) S265–S273 doi:10.1088/0960-1317/17/9/S09

An autonomous CO_2 discharge and electrolyte agitation scheme for portable microbial fuel cells

Chien-Chou Chen and Yu-Chuan Su

Department of Engineering and System Science, National Tsing Hua University, Taiwan

E-mail: ycsu@ess.nthu.edu.tw

Received 26 February 2007, in final form 28 June 2007
Published 31 August 2007
Online at stacks.iop.org/JMM/17/S265

Abstract

We have successfully demonstrated a passive scheme that employs interfacial tensions to discharge a CO_2 by-product out of portable microbial fuel cells (MFCs). The MFCs consume glucose to generate electricity and CO_2 gas in a reaction catalyzed by encapsulated microorganisms. The bio-catalysts, fuels and electrolytes are sealed inside two liquid-impermeable compartments, which are separated by a proton exchange membrane. The discharge of unwanted CO_2 bubbles from a closed anode compartment could result in desired agitation, which significantly facilitates the electron transport to the anode electrode. In our experiment, a MFC with a projected electrode area of 1 cm^2 and an overall size of $30 \times 15 \times 5$ mm^3 was built. It was demonstrated that an open-circuit voltage of roughly 0.37 V per unit and a 1 h average power output up to 32 $\mu W\ cm^{-2}$, which is five times a regular-sized MFC, were achieved by the proposed discharge and agitation mechanism. With 40 mg of glucose fuels, the miniature MFC continuously operated for up to 4 h. Furthermore, a fuel-cell plate of six units, which had an overall open-circuit voltage over 2 V, was built and successfully powered a light-emitting diode. As such, the proposed discharge and agitation mechanism could self-regulate the electricity harvesting inside a MFC and produce steady voltage and current outputs for portable applications.

(Some figures in this article are in colour only in the electronic version)

Introduction

Fuel cells are electrochemical energy-conversion devices that produce electricity from supplies of fuels and oxidants. A variety of fuel cells with different physical structures and fuel-oxidant combinations are currently being developed [1, 2]. It has been demonstrated that fuel cell reactions are more efficient, as well as cleaner, quieter and safer than most existing energy-conversion schemes [3]. Furthermore, fuel cell reactions can extract energy from a variety of renewable sources. It is therefore anticipated that fuel cells will be one type of major energy source to power the world in the future. However, the high cost of fuel cells, especially on expensive platinum catalysts, is the most significant disadvantage that severely limits the further adaptation of fuel cells [4].

The concept of using microorganisms as catalysts in fuel cells, known as microbial fuel cells (MFCs), has been explored since the 1970s [5–7]. MFCs are capable of converting chemical energy, which is available in bio-convertible substrates, directly into electrical energy. By replacing expensive catalysts with naturally occurring microorganisms to promote the oxidation of electron donors, the manufacturing cost of MFCs is much lower than that of conventional ones. Potentially, MFCs could supply electricity for a variety of applications and help fulfill the increasing demand for energy [8]. More importantly, they are promising in powering life-supporting implantable medical devices, which need to work inside biofuel-abundant bodies for a long period of time [6]. Previously, various combinations of microorganisms and mediators have been demonstrated to be functional as

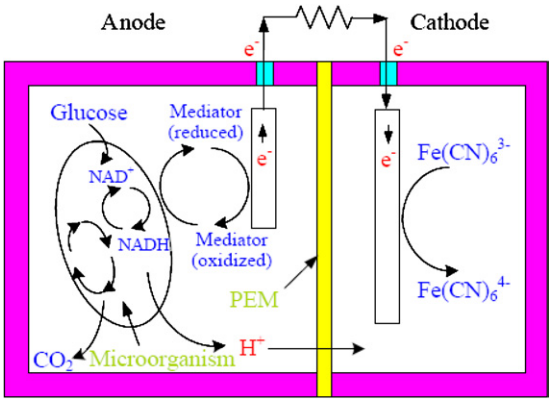

Figure 1. Working principle of a mediator-assisted microbial fuel cell.

biocatalysts [9–11]. In some instances, microorganisms might even produce their own mediators to promote extra-cellular electron transfer [12, 13]. Furthermore, researchers have demonstrated micromachined MFCs that function for a short period of time [14]. Since there is no fuel circulating or supplying component in these cells, their probable working period is severely limited. For long-term operation, an automatic control system (preferably passive) is required to regulate the mass transfer of reactants and products in and out of the reactor.

To address this need, this work presents a passive scheme that can autonomously discharge CO_2 bubbles and agitate aqueous anolyte to enhance the electricity generation inside portable MFCs. The proposed MFC has breathable compartments, which are impermeable to liquids but permeable to gases. Driven by interfacial tensions, the generated CO_2 gas is continuously released out of the anode compartment and water vapor can diffuse out of the compartment as well. Compared to existing large-sized MFCs, three accomplishments have been achieved: (1) autonomous discharge of unwanted CO_2 bubbles, (2) portability and prolonged working period and (3) improvement in charge transport and current output caused by autonomous agitation. As such, the proposed MFC is capable of self-regulating the electricity harvesting process and producing steady outputs for an extended period of time.

Operation principle

Microorganism catalysis

Figure 1 shows the working principle of a mediator-assisted MFC. In this work, Saccharomyces cerevisiae (baker's yeast) was employed as the bio-catalyst to oxidize glucose, while hydrogen protons, electrons and carbon dioxide were generated through the reaction. Yeast is a facultative anaerobe that can live in the absence as well as in the presence of atmospheric oxygen. In either microbial catabolism, electrons are released by enzymatic reactions and stored as reduced intermediates. In the absence of oxygen, electrons may be diverted from the respiratory chain by an oxidation-reduction mediator. Mediators, sometimes referred to as electron shuttles, are capable of crossing cell membranes, accepting electrons from one or more electron carriers within cells, exiting cells in the reduced form and then transferring electrons onto the electrode surface [15, 16]. In principle, mediator molecules collect electrons from biological electron transport chains of microorganisms and transport them to electrodes of MFCs. In addition, protons are driven across a proton exchange membrane (PEM) by diffusion. Inside the cathode compartment, the catholyte is a solution of potassium ferricyanide, which accepts electrons and reduces to ferrocyanide, in potassium phosphate buffer. Overall, the reaction consumes glucose while producing carbon dioxide and water. By diffusion, the reduced electron mediators travel through the buffer solution and eventually deposit their electrons on the anode.

CO_2 discharge and electrolyte agitation

Most of the existing large-sized MFCs have open compartments, such that reactant and by-product gases can flow in and out freely. To promote the charge transport in MFCs, it is common to use externally supplied power to agitate the electrolytes. For MFCs to be portable, however, the liquid electrolytes need to be sealed in the compartments and the power consumption should be minimized to extend their working periods. Furthermore, in order to prevent the build-up of pressure that eventually degrades the system, CO_2 by-product must be efficiently discharged from the anode compartment. Generally, bubbles can be removed by hydrophobic gas vent if the electrolyte is a simple gas/liquid mixture [17]. With proper design, it is therefore feasible to employ the built-up gas pressure as a power source to drive CO_2 bubbles, cause desired agitation and discharge CO_2 by-product passively and smoothly. The key component to achieve these is a patterned graphite electrode. As indicated in figure 2, CO_2 gas is generated inside the gap between the PEM and the graphite electrode, and eventually merges to form tiny bubbles. Some of them will randomly move out of the gap, but most of them will stick on the surfaces if there is no extra driving force. While CO_2 bubbles are entrapped inside the gaps, capillarity could act to generate a desired pressure gradient, which can passively guide the movement of these bubbles. As shown in figure 3(*a*), a hydrophilic gap diverging from left to right will apply a pressure gradient along this direction to an entrapped bubble. Right before the bubble escapes from the gap, the ratio of R_c to R_0 is estimated to be

$$\frac{R_c}{R_0} = \frac{2\cos\theta}{\cos\theta + \cos(\theta - \varphi)}, \tag{1}$$

where R_c and R_0 are the radii of the curved interface at the opening and inside the gap, respectively, ϕ is the wall angle of the electrode and θ is the contact angle between anolyte, CO_2 gas and the electrode surface. Based on the Young–Laplace equation, the pressure difference across an interface can be determined by the tension and shape of the interface [18]. Therefore, it is expected that an electrode with a wall angle ϕ equal to θ will have the highest pressure gradient to drive bubbles out of the gap.

After escaping from the diverging gap, CO_2 bubbles will accumulate and eventually expand into the through holes on

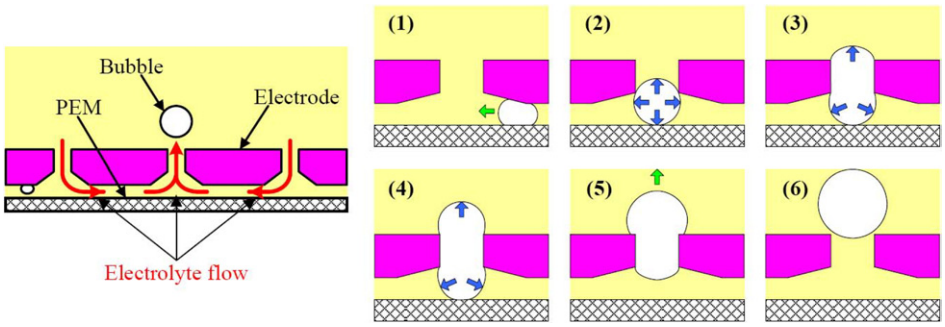

(*a*) (*b*)

Figure 2. (*a*) Autonomous electrolyte agitation caused by bubble discharging and (*b*) a complete sequence of bubble discharging.

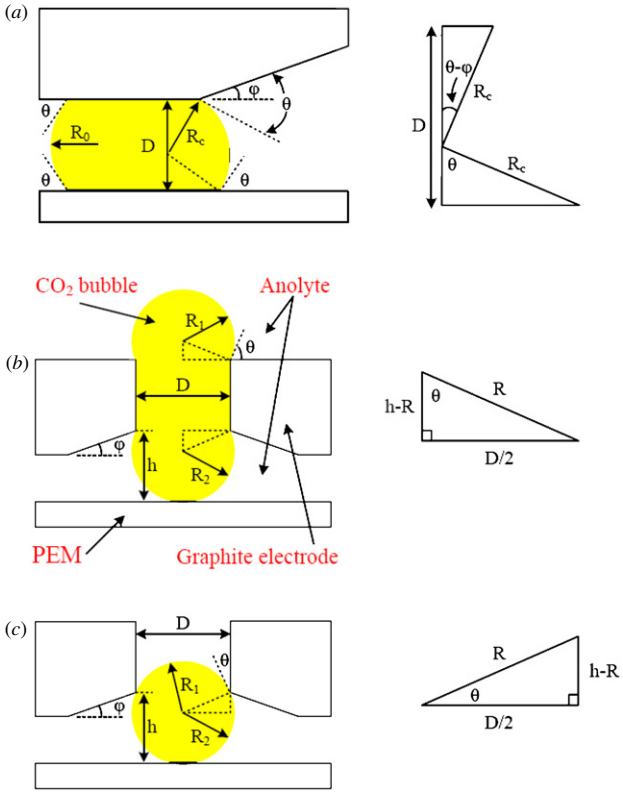

Figure 3. Geometries of a CO_2 bubble right before it is (*a*) driven out of a gap, (*b*) discharged from a graphite electrode and (*c*) driven into a through hole on the electrode.

the graphite electrode (as shown in figure 2(*b*)(2)). Since the dimension of these holes is larger than that of the hydrophilic gap, bubbles will expand along the holes until they reach the other side of the electrode. Once a bubble reaches the top-side exit, a pressure barrier built by the abruptly diverging opening will temporally prevent the bubble from continuously expanding upwards. Restrained by the pressure barrier, the inner pressure of the bubble will keep rising until it exceeds the barrier pressure. Meanwhile, the bubble may expand further into the bottom gap and stopped by the pressure barrier set by the converging shape. Figure 3(*b*) shows the geometry of a CO_2 bubble right before it is discharged from a graphite electrode. At this moment, the CO_2 pressure reaches its maximum, which is just enough to overcome the pressure barrier built at the opening. Related by the contact angle, the geometries of the gas–liquid interface and the through-hole can be described as

$$\frac{D/2}{R} = \sin\theta \qquad \text{and} \qquad \frac{D}{R} = 2\sin\theta, \tag{2}$$

where R is the radius of the curved interface and D is the diameter of through hole. Since the top and bottom interfaces have the same interfacial tension and pressure difference, the radii of the two curved interfaces should be equal. To simplify the derivation, it is assumed that the lower portion of the bubble makes only point contact with the PEM. As such,

$$\frac{h-R}{R} = \cos\theta \qquad \text{and} \qquad \frac{h}{R} = 1+\cos\theta, \tag{3}$$

where h is the height of the gap between the PEM and graphite electrode. Therefore, the relationship between the gap height (h) and hole diameter (D) can be described as

$$\frac{h}{D} = \frac{1+\cos\theta}{2\sin\theta}. \tag{4}$$

Similarly, the geometry of a CO_2 bubble right before it is driven into a through hole (as shown in figure 3(*c*)) can be analyzed and the result can be described as

$$\frac{h}{D} = \frac{1+\sin\theta}{2\cos\theta}. \tag{5}$$

After overcoming the pressure barrier, the inner pressure abruptly drops and the bubble expands upwards. At the same time, the bubble will recede from the converging gap, and detach from the PEM surface because of the reduction in the interfacial curvature (as shown in figure 2(*b*)(5)) caused by the pressure drop and buoyant force as well. After that, the bubble will escape from the through hole because of the actuation of capillary and buoyant forces. The vacancy left behind will result in a refill of electrolyte, which agitates the fluid around the electrode and facilitates electron transport to the electrode (as shown in figure 2(*a*)). The CO_2 bubble will float upwards and finally penetrate the hydrophobic porous membrane. As such, spontaneous discharge and agitation can be achieved simply by buoyancy and interfacial tensions without any external power consumption.

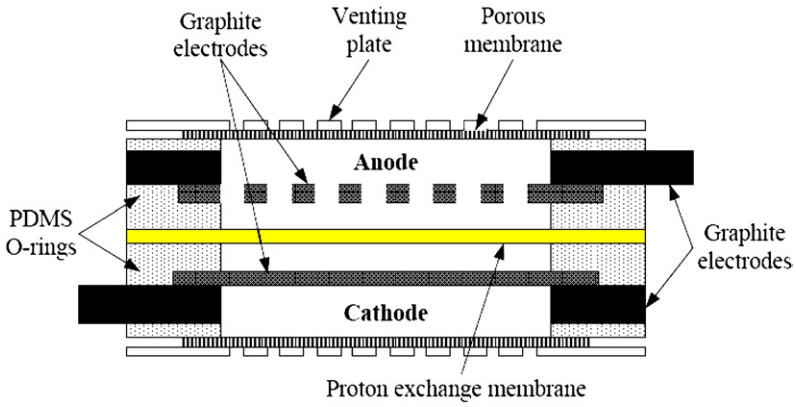

Figure 4. Schematic of a portable microbial fuel cell with breathable compartments.

MFC design

A schematic of the proposed portable MFC is shown in figure 4. A patterned graphite electrode with through holes is placed in the middle of the anode compartment. CO_2 bubbles are driven to flow through these holes and both top and bottom surfaces of the electrode plate are exposed to aqueous electrolytes. As such, the effective area for electron transfer is almost doubled. On top of the anode compartment, a hydrophobic porous membrane is employed not only to seal the liquid electrolyte inside but also to provide a discharge pathway for the CO_2 by-product. Driven by buoyancy, a CO_2 bubble will float up and accumulate underneath the porous membrane, which has micro-scale hydro-phobic through pores on it. Because of capillarity, the aqueous electrolyte is prevented from penetrating the membrane, but gases are allowed to flow through. Furthermore, these small pores also assist encapsulate yeasts inside the anode compartment. To support the thin membrane, a venting plate with an array of through holes will be mounted as the cover of the MFC. Similar design is applied to the bottom-half cathode compartment as well.

Fabrication process

An assembly diagram of the proposed MFC, which is composed of polymeric parts and graphite electrodes, is shown in figure 5. Polymethylmethacrylate (PMMA) plates (ACRYREX, Chi Mei) shaped by micro-milling were used as the main structures for mechanical support and assembly. On these plates, there are arrays of small through holes designed for gas breathing. Hydrophobic polytetrafluoroethylene (PTFE) membranes (ADVANTEC J100A025A), which have a pore size of 1 μm, were pressed on these through holes to form liquid-impermeable pathways for CO_2 discharge. On the other hand, soft polydimethylsiloxane (PDMS, Sylgard 184, Dow Corning) o-rings were cast and sandwiched between adjacent structural layers to achieve reliable sealing, which is necessary in order to sustain the high pressure caused by CO_2 accumulation. Finally, the required clamping forces to hold this multi-layer structure were realized by the friction between the screw and PMMA surfaces.

Dupont Nafion-117 thin film was chosen as the PEM material because of its unique selective-permeable property. It

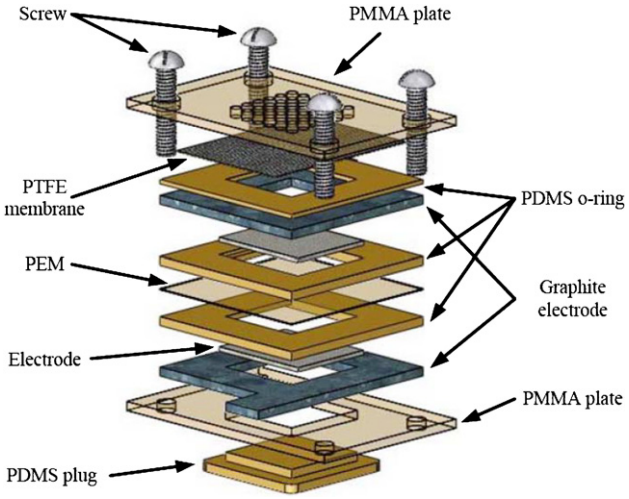

Figure 5. Assembly diagram of a prototype microbial fuel cell.

was sliced into a 15 × 15 mm^2 film and cleaned in boiling H_2O_2 and H_2O solutions to remove the contaminations on its surfaces before being sandwiched between PDMS o-ring layers. The working electrodes for electron collection could be made of either carbon cloth or graphite plates as shown in figure 6. If carbon cloth was used, the effective electrode areas were notably magnified because of the weaved textures. However, it will be difficult to further shape carbon cloth into specific three-dimensional structures, which can facilitate the movement and discharge of CO_2 bubbles. Comparatively, graphite plates can be conveniently shaped by either hot embossing or precise milling to form microscale pattern on their surfaces. A patent-pending graphite-polymer composite material, which was provided by a research group also in National Tsing Hua University, was employed to fabricate the electrodes. First, the graphite-polymer composite material was molded into 25 × 25 × 1 mm^3 plates at high temperature. Afterwards, the through holes and inclined surfaces (as shown in figures 2 and 6) that drive CO_2 bubbles moving across electrodes were fabricated by a two-step milling process. In this process, an electrode was first machined using a ball end mill (with 2 mm in radius) to form an array of 2.7 mm spacing spherical cavities on one surface. After that, a smaller flat end mill

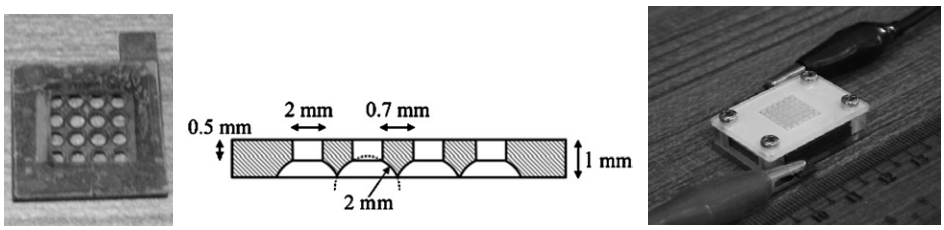

Figure 6. Photographs of (*a*) a graphite electrode and (*c*) the prototype microbial fuel cell, and (*b*) cross-sectional view of the graphite electrode.

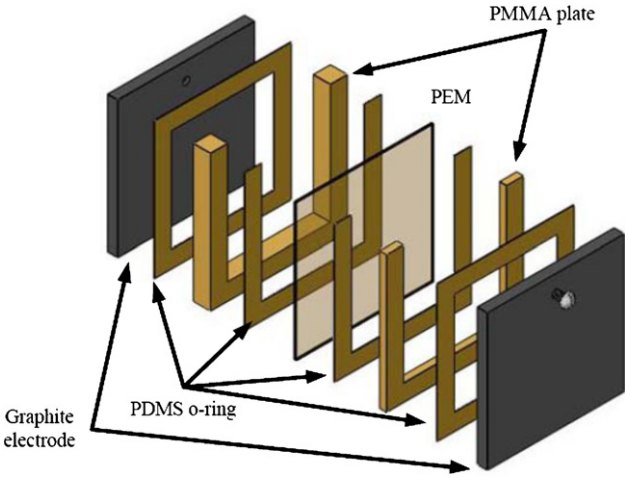

Figure 7. Assembly diagram of a large-sized reference microbial fuel cell.

(with 1 mm radius) was used to drill concentric through holes from the other surface. For prototype demonstration, graphite electrodes with 1 cm^2 projected electrode area were fabricated as shown in figure 6. Once the components were aligned and packed accordingly, the MFC was assembled using screws to provide the required clamping forces. A prototype system having an overall size of 30 × 15 × 5 mm^3 is shown in figure 6. Furthermore, a large-sized MFC with a 9 cm^2 projected electrode area (shown in figure 7), which was made of the same materials as the miniature one, was also built and employed as a reference for comparison.

Experimental details

Sample preparation

The microorganism used in our experiments was Saccharomyces cerevisiae, which was purchased from a local bakery in wet form and stored at 4 °C before used. First, the microorganisms were hydrated and re-activated in a phosphate buffer (0.1 M and pH 7.0) for 30 min. For anolyte, the microorganisms were mixed with glucose in various concentrations. An electron transfer mediator, methylene blue (0.01–0.05 M), was added to promote the energy conversion efficiency. The catholyte, a potassium ferricyanide solution at 0.02 M, was also prepared in a phosphate buffer (0.1 M, pH 7.0). Mixtures of various concentrations of yeasts, glucose and methylene blue were tested. According to published data [16, 19] and our tests, it was found that a mixture of 0.1 g ml^{-1} yeast, 1 M glucose and 0.05 M methylene blue in 0.1 M phosphate buffer (pH 7.0) has the highest current output among similar conditions. Therefore, all the following experiments were performed with this same composition to compare the performance of different fuel-cell configurations. An anolyte of an overall volume of 0.25 ml and catholyte of 0.4 ml were dispensed into the anode and cathode compartments, respectively, and assembled into a final form as shown in figure 6. The packed MFC was then incubated at 40 °C in an oven for 30 min before further electrical measurements (also at 40 °C) were performed. For the large-sized reference MFC, the same electrolytes with a volume of 1.8 ml each were dispensed into its anode and cathode compartments, which are open to the atmosphere for O_2 supply and CO_2 discharge.

CO_2 discharge

The growth and discharge of CO_2 bubbles from the anode compartment were observed and recorded under optical microscopes. A half cell (only the anode compartment) was immersed in a glass petri dish filled with de-ionized water (as shown in figure 8), so the CO_2 gas evolved from the anode compartment can be clearly monitored by a top-side microscope (OM 1). From the bottom optical microscope (OM 2), the growth and movement of CO_2 bubbles in the gap between the PEM and the graphite electrode were observed. Since the anolyte is opaque, the through holes on the graphite electrode can only be observed through CO_2 bubbles, which appear as black spots in the figure. The white spots are actually the through holes on the graphite electrode with a white porous membrane on the background. For reference, the white circles in figure 8(*b*)(1) indicate the positions of these through holes. By analyzing the images grabbed by the bottom-side microscope, the electrode area available for electron transport can be estimated.

Output characterization

In this work, the performance of a MFC was evaluated by its open-circuit voltage (OCV) and current outputs. Each prototype was filled with the same electrolyte (as mentioned previously), assembled and electrically connected for testing. The OCV and current outputs were monitored by a digital multi-meter (Agilent 34405A) over a certain period of time. For output current measurement, the prototype MFC was connected with a 1000 Ω resistor in series. In order to

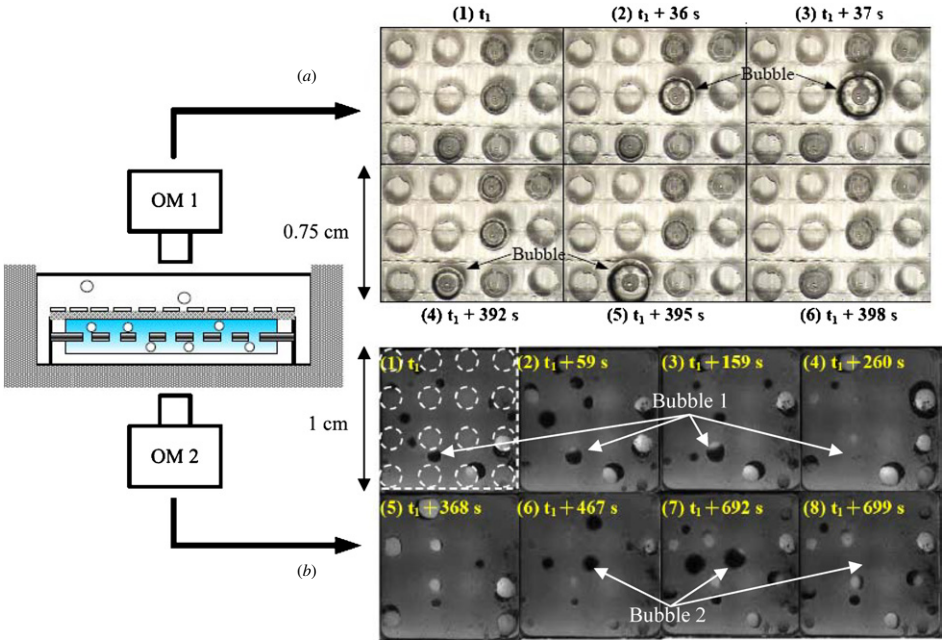

Figure 8. Images of CO_2 bubbles discharging from a half cell (*a*) taken above a venting plate and (*b*) recorded underneath a graphite electrode.

compare the current and power outputs from prototypes with different dimensions, the outputs were further normalized by their electrode areas. Throughout the testing period, prototype MFCs were placed horizontally (with anode on top of cathode) in a incubator (at 40 °C) without any external disturbance.

Results and discussion

Figure 8 shows the sizes and distribution of CO_2 bubbles while a functional gas-discharge scheme was implemented in a half MFC. Throughout the bio-catalyzed reaction, CO_2 gas was continuously generated (in a rate estimated to be roughly 0.03 ml min^{-1} with 1 ml of anolyte at 1 atm) and accumulated inside the anode compartment. Generally, CO_2 bubbles tend to stick on surfaces and grow (or merge together) into larger bubbles. If CO_2 gas was not discharged properly, eventually it occupied the whole space and ejected the anolyte out of the anode compartment. Consequently, the bio-catalyzed reaction was terminated. In contrast, a passive gas-discharge scheme prolonged the operation or even enhanced the performance of a MFC. From the photographs taken underneath a graphite electrode (as shown in figure 8), it was observed that CO_2 bubbles accumulated at specific positions and floated across the graphite electrode once their volumes reached certain limits. For example, bubbles 1 and 2 remained at the same position and growing for roughly 5 min before they floated out and disappeared. The vacancy was refilled right away by an induced flow parallel to the electrode surface. At the same time, it was observed from the top side that CO_2 bubbles were periodically discharged across a hydrophobic porous membrane. In just a few seconds, CO_2 bubbles suddenly emerged and floated up into the environment. Furthermore, there was no sign of colorful anolyte leaking across the membrane. All these results indicate that effective

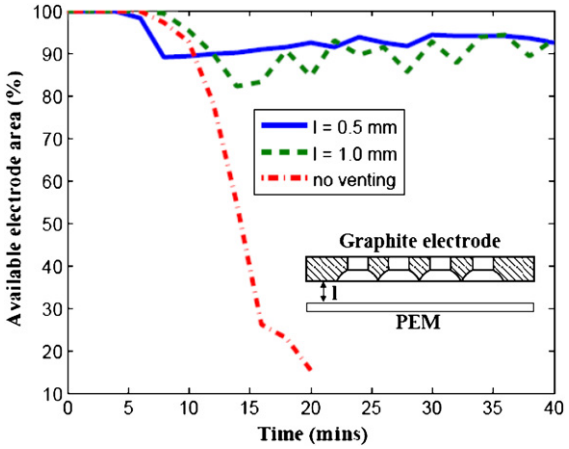

Figure 9. Fluctuation of the available electrode area while various configurations were employed.

CO_2 discharge was achieved by the proposed scheme, which was powered by CO_2 pressure and capillary forces.

The interactions between CO_2 bubbles and the structure (especially the graphite electrode and the membranes) are critical to the performance of a MFC. For example, the covering of CO_2 bubbles on the electrode surface actually obstructs the transport of electrons and lowers the output current. Figure 9 shows the fluctuations of available electrode areas while various cell structures were employed. It was found that the discharge of CO_2 bubbles from a smaller gap (0.5 mm) was more frequent and the discharged bubbles were smaller. The reason is that bubbles in a smaller gap experienced higher capillary pressure gradients, which tend to drive them out of the gap and shorten their stay on the electrode surface. The larger bubbles in a wider gap were more likely to block bigger electrode areas for longer time so the resulted

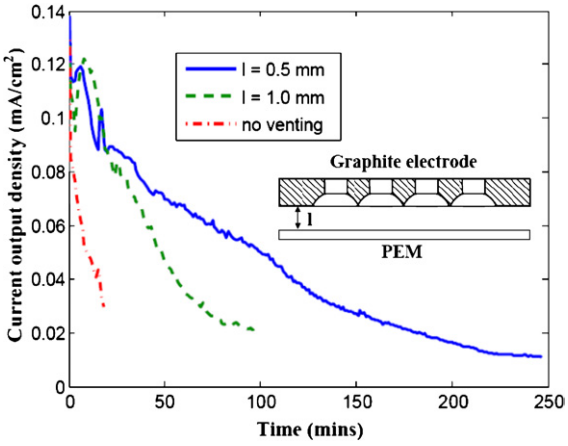

Figure 10. Time-varying current output of prototype fuel cells with various electrode configurations.

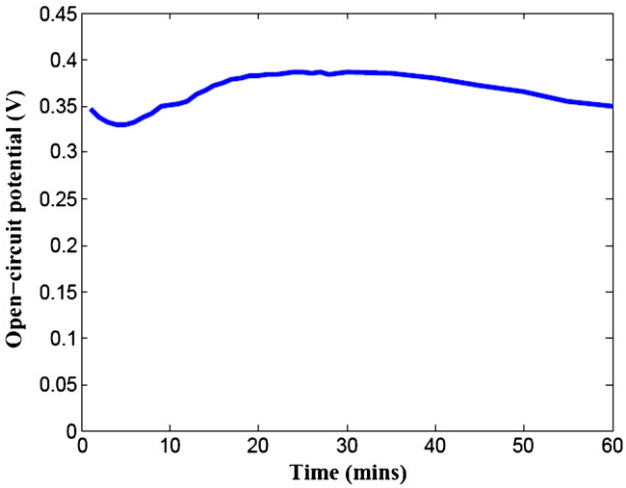

Figure 11. Open-circuit potential of a prototype microbial fuel cell.

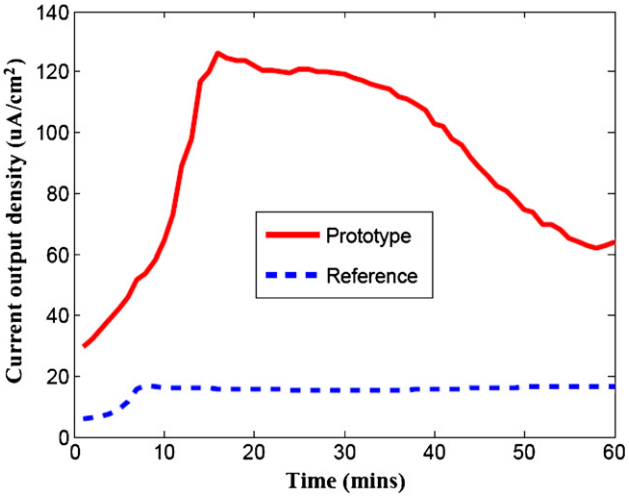

Figure 12. Comparison of current outputs from prototype and reference microbial fuel cells.

fluctuation was higher and the average available electrode area was lower. The induced electrolyte flow also resulted in the agitation of anolyte inside the compartment, which notably facilitated the transfer of electrons. Since CO_2 gas was homogenously generated at a fixed rate and all discharged from the gap, the agitation caused by bubble flow was expected to be about the same in both narrow and wide gaps. Figure 10 illustrates the current outputs from three cell structures with different discharge and agitation characteristics. It was found that the one that had the best discharge performance also had the highest current output. In our experiment, the contact angle between anolyte, bubble and solid (either electrode or PEM) surface was roughly 67°, and the graphite electrode had a wall angle of roughly 43°. Predicted by equations (4) and (5), the maximum h/D ratio for CO_2 discharge is roughly 0.76 and that for penetration is roughly 2.46. For structures with h/D ratios higher than 0.76 (for example while $l = 1$ mm), CO_2 bubbles leaned against the PEM and expanded into the gap. If the minimum height of the gap was smaller than the diameter of the through hole, eventually bubbles might still be expelled and discharged from the through hole. In general, hydrophilic electrodes with smaller through holes and even smaller gaps are preferred. For the cell structure with $l = 0.5$ mm, its operation period was extended to more than 4 h. At the end, the operation was terminated probably because of microorganism self-pollution, substrate deficiency, or the toxic effects caused by chemical mediators. For cells with limited discharge capacities (with bubble removal rates lower than generation rates), eventually the accumulated bubbles would still cover the whole electrode surface and terminate the MFC reactions after short periods.

In addition to current output, the open-circuit voltage of our miniature MFC was also measured and the result is shown in figure 11. The OCV was relatively stable in a range from 0.32 V to 0.4 V over a 1 h period. Compared to published data [14, 16, 19], the measured OCV values are lower because of the Ohmic resistance loss and potential electrolyte leakage in our current prototype. In order to evaluate the enhancement achieved by spontaneous discharge and agitation, the current outputs from a miniature prototype and a large-sized MFC were compared as shown in figure 12. With exactly the same electrode materials, electrolytes, fuels, microorganisms and reaction conditions, only the geometries and flow behaviors inside the anode compartment will cause the variation in current outputs. Compared to the large-sized reference MFC, the prototype had higher current output, which reached 120 μA cm^{-2} around 20–30 min and dropped to 60 μA cm^{-2} after 60 min. The power output was estimated to be 32 μW cm^{-2} in the first hour, which is five times of a regular large-sized one. However, the output of a regular one was obviously more stable over time because of its larger electrode area. It is expected that with reduced feature sizes, the performance and stability of the proposed MFC could be further improved.

For most applications, an OCV of 0.37 V is too low to support their operations. In order to achieve higher voltage output, plates of MFCs connected in series were built and characterized. Figure 13 shows the assembly diagram and photograph of a demonstrated six-unit fuel cell plate with an overall dimension of 60 × 45 × 5 mm^3. It has been demonstrated that with six proposed cells connected in series, the output, which is illustrated in figure 14, is capable of powering a LED for a short period of time.

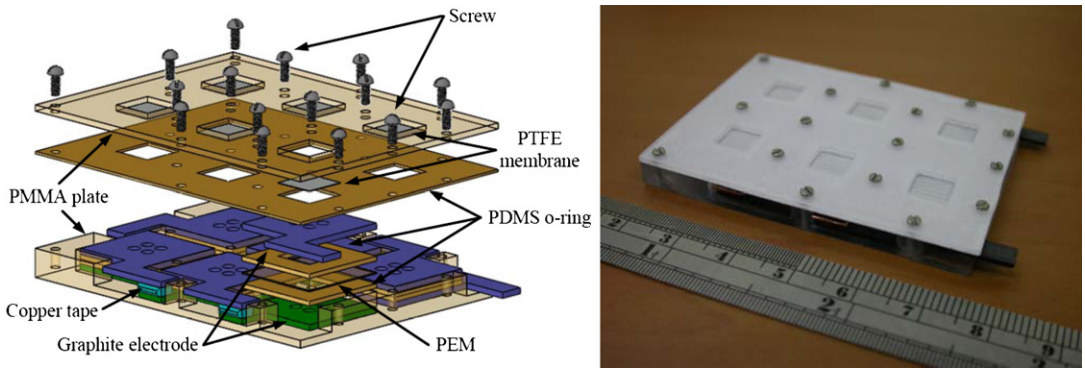

Figure 13. Assembly diagram and photograph of the demonstrated six-unit fuel cell plate.

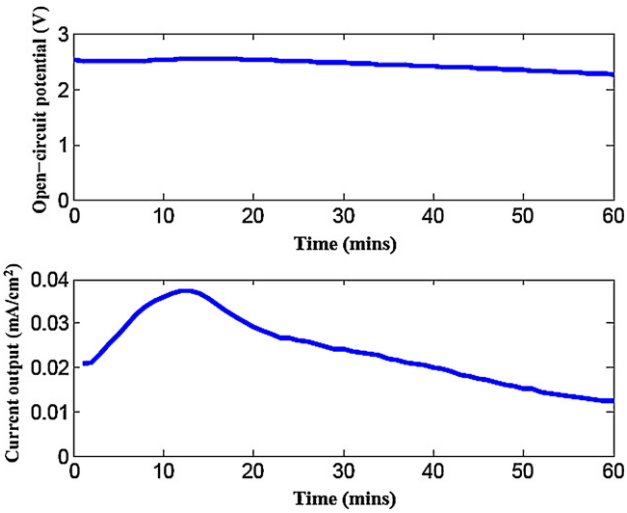

Figure 14. Output characteristics of the demonstrated six-unit fuel cell plate.

Conclusion

In this work, a discharge and agitation scheme for portable microbial fuel cells (MFCs) has been successfully demonstrated. The demonstrated MFC consumes glucose to generate electricity and CO_2 in a reaction catalyzed by encapsulated Saccharomyces cerevisiae. Throughout the reaction, the unwanted CO_2 by-product is autonomously discharged by a bubble guiding and venting sub-system, which periodically releases the built gas pressure and agitates the electrolyte inside the anode compartment as well. In the experiments, an open-circuit voltage at around 0.37 V per unit and an average power output of 32 μW cm^{-2} in the first hour were achieved. With 40 mg of glucose fuels, the miniature MFC continuously operated for up to 4 h. Furthermore, a fuel-cell plate of six units, which has an overall open-circuit voltage over 2 V, was built and successfully powered a light-emitting diode. Eventually, the operation was terminated probably because of microorganism self-pollution, substrate deficiency, or the toxic effects caused by chemical mediators. To overcome these potential threats, further regulating mechanisms need to be developed and integrated. After all these efforts, MFCs will be capable of self-regulating the electricity harvesting process and producing steady voltage and current outputs for portable applications.

Acknowlegments

The authors would like to express their appreciation to Professor Chen-Chi Ma and his research group for providing the graphite-polymer composite for MFC construction. This work was supported in part by the National Science Council of Taiwan under contract no. NSC 93-2212-E-007-057. The demonstrated systems were fabricated in the ESS Microfabrication Lab at National Tsing Hua University, Taiwan.

References

[1] Steele B C H and Heinzel A 2001 Materials for fuel-cell technologies *Nature* **414** 345–52
[2] Winter M and Brodd R J 2004 What are batteries, fuel cells, and supercapacitors? *Chem. Rev.* **104** 4245–69
[3] Larminie J and Dicks A 2003 *Fuel Cell Systems Explained* (Chichester: Wiley)
[4] Srinivasan S 2006 *Fuel Cells: From Fundamentals to Applications* (New York: Springer)
[5] Palmore G T R and Whitesides G M 1994 Microbial and enzymatic biofuel cells *Enzymatic Conversion of Biomass for Fuel Production* (Washington, DC: American Chemical Society)
[6] Katz E, Shipway A N and Willner I 2003 Biochemical fuel cells *Handbook of Fuel Cells* (New York: Wiley)
[7] Bullen R A, Arnot T C, Lakeman J B and Walsh F C 2006 Biofuel cells and their development *Biosens. Bioelectron.* **21** 2015–45
[8] Lovley D R 2006 Bug juice: harvesting electricity with microorganisms *Nat. Rev. Microbiol.* **4** 497–508
[9] Roller S D, Bennetto H P, Delaney G M, Mason J R, Stirling J L and Thurston C F 1984 Electron-transfer coupling in microbial fuel cells: I. Comparison of redox-mediator reduction rates and respiratory rates of bacteria *J. Chem. Tech. Biotechnol.* **34B** 3–12
[10] Delaney G M, Bennetto H P, Mason J R, Roller S D, Stirling J L and Thurston C F 1984 Electron-transfer coupling in microbial fuel cells: II. Performance of fuel cells containing selected microorganism-mediator-substrate combinations *J. Chem. Tech. Biotechnol.* **34B** 13–27
[11] Park D H and Zeikus J G 2000 Electricity generation in microbial fuel cells using neutral red as an electronophore *Appl. Environ. Microbiol.* **66** 1292–7
[12] Newman D K and Kolter R 2000 A role for excreted quinones in extracellular electron transfer *Nature* **405** 94–7
[13] Hernandez M E, Kappler A and Newman D K 2004 Phenazines and other redox-active antibiotics promote microbial mineral reduction *Appl. Environ. Microbiol.* **70** 921–8

[14] Chiao M, Lam K B and Lin L W 2006 Micromachined microbial and photosynthetic fuel cells *J. Micromech. Microeng.* **16** 2547–53
[15] Bennetto H P, Stirling J L, Tanaka K and Vega C A 1983 Anodic reactions in microbial fuel cells *Biotechnol. Bioeng.* **25** 559–68
[16] Bennetto H P 1990 Electricity generation by microorganisms *Biotechnol. Educ.* **1** 163–8
[17] Meng D D, Kim J and Kim C-J 2006 A degassing plate with hydrophobic bubble capture and distributed venting for microfluidic devices *J. Micromech. Microeng.* **16** 419–24
[18] Adamson A W and Gast A P 1997 *Physical Chemistry of Surfaces* (New York: Wiley)
[19] Walker A L and Walker C W 2006 Biological fuel cell and an application as a reserve power source *J. Power Sources* **160** 123–9